Development of a Mechanistic Condensation-Liquid Film Coupled Model and Its Application to Forced-Convection Condensation of Superheated Steam

Hyung Jun Kim[a], Jeong Hun Kang[a], Jia Yu[b], Yeon-Gun Lee[a*]
[a]*Department of Quantum and Nuclear Engineering, Sejong University, 209, Neungdong-ro, Gwangjin-gu, Seoul, Republic of Korea*
[b]*Digital Solution Research Department, KEPCO E&C, 269, Hyeoksin-ro, Gimcheon-si, Gyeongsangbuk-do, 39660, Republic of Korea*
[*]*Corresponding author: yglee@sejong.ac.kr*

***Keywords :** Passive heat sinks, Mechanistic condensation model, Liquid film model, Superheated steam

1. Introduction

Under design extension conditions in containment buildings, wall condensation is a key phenomenon that governs the pressure and temperature behavior as well as the heat removal from the containment. Particularly when the containment spray system fails due to multiple failures, passive heat sinks such as the liner plate and concrete walls become virtually the only means of heat removal. Therefore, it is essential to secure an analytical model capable of precisely predicting the heat transfer due to wall condensation of the steam-air mixture. However, conventional condensation analyses have often neglected the effect of the liquid condensate or relied on the simplified film model such as the Nusselt model [1].

Because the Nusselt model is derived for pure steam condensation, the mass flow rate and thickness of film will be overestimated when it is applied to environments containing noncondensable gases. In addition, many variables associated with turbulence in the vapor-gas boundary layer are influenced by the condensate velocity at the interface. Hence, a mechanistic liquid film model that considers the effect of the interfacial shear stress is required to improve the predictive accuracy for steam condensation on passive heat sinks.

Furthermore, during the early stages of accidents like a Main Steam Line Break (MSLB), the containment atmosphere can be exposed to superheated steam conditions [2]. When superheated steam condenses, the heat removal at the wall is not solely governed by the latent heat of condensation, but also involves the removal of sensible heat as the superheated steam cools to a saturated state. In addition, non-condensable gases such as air form a diffusion resistance layer near the interface, suppressing condensation. Under superheated conditions, the net condensate rate may further decrease due to re-evaporation [3]. Therefore, there is a need for a modeling framework that consistently couples steam condensation with liquid film behavior, and enables its application to superheated steam condensation.

In this study, a liquid film model was implemented into a mechanistic condensation model for forced-convection flow over a vertical plate [4]. The coupled model was subsequently extended to predict superheated steam condensation by accounting for changes in the condensate mass flow rate relative to the saturated state. The mechanistic coupled model was validated against three sets of forced-convection condensation tests.

2. Model

Fig. 1 shows an overview of the schematic diagram of the condensation model in a superheated steam–air mixture field. Along the cooled wall, a thin condensate film is formed and flows downward in the direction of gravity, and outside the film, a vapor boundary layer and a liquid–vapor interface exist. The flow of the condensate film is in the x-direction, and a portion of the mass condenses at the interface and enters the film by an amount of $d\dot{m}^*$, so that the mass flow rate is corrected to $\dot{m} + d\dot{m}^*$. The transferred heat flux (q_s'') is divided into two parts: the latent heat term (dq_{cond}) due to condensation and the sensible heat term (dq_{conv}) associated with cooling from the bulk mixture temperature (T_b) to the interfacial temperature (T_i). In other words, under superheated conditions, this figure schematically illustrates that both the latent heat released by condensation and the sensible heat due to cooling of the superheated steam are transferred to the wall.

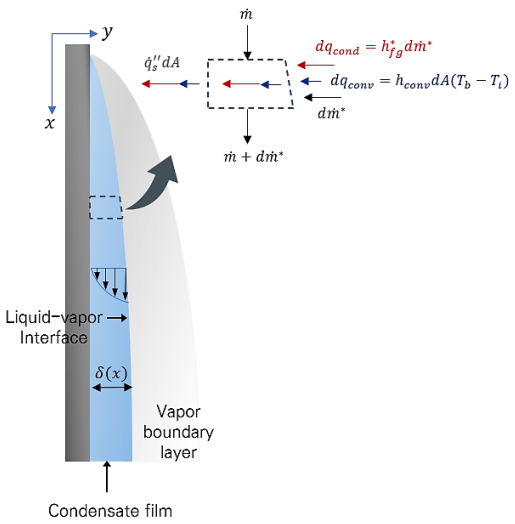

Fig. 1. Solution of the coupled condensation-liquid film

2.1 Condensation model

The mechanistic condensation model developed in the previous study [4] calculates the interfacial condensation mass flux based on the mass transfer of the steam component in a steam-non-condensable gas mixture. Since it is difficult to describe the diffusion intensity solely with molecular diffusion in turbulent flow, this model employs an effective diffusion coefficient that combines molecular diffusion and turbulent diffusion. The effective diffusion coefficient is defined as follows:

$$D_{eff} = D_m + D_T \tag{1}$$

where D_{eff} is the effective diffusion coefficient, D_m is the molecular diffusion coefficient, and D_T is the boundary layer average of the turbulent diffusion coefficient.

In the inner region of the boundary layer, the turbulent diffusion coefficient is calculated using the mixing length and velocity gradient as follows [5]:

$$D_T = l_m^2 \left|\frac{\partial \bar{u}}{\partial y}\right| \tag{2}$$

where l_m is the mixing length [6], $\bar{u}$ is the time-averaged streamwise velocity, and y is the distance from the wall.

Conversely, in the outer region of the boundary layer, the following empirical formula is used [6]:

$$D_T = \frac{0.0168 U_\infty \delta_1}{\left[1 + 5.5.\left(y/\delta_g\right)\right]} \tag{3}$$

where U_∞ is the free stream velocity, δ_1 is the displacement thickness of the boundary layer, and δ_g is the thickness of the gas boundary layer.

Next, the mass transfer coefficient is expressed in terms of the Sherwood number. Since turbulent diffusion is already reflected in D_{eff}, this model uses the modified Sherwood number Sh^* correlations. For the laminar and turbulent regimes, the following equations are applied, respectively [7]:

$$Sh^*_{x,l} = 0.601 Re_x^{0.422} Sc^{1/3} \tag{4}$$
$$Sh^*_{x,t} \cdot x^{0.272} = 4.03 Sh^*_{x,l} \tag{5}$$

where $Sh^*_{x,l}$ and $Sh^*_{x,t}$ are the modified Sherwood numbers for laminar and turbulent flows respectively, Re_x is the Reynolds number based on the distance from the inlet x, and Sc is the Schmidt number.

Finally, the condensation mass flux at the interface is calculated as follows:

$$\dot{m}''_{v,i} = Sh^* \frac{D_{eff}}{x} \left(\frac{\rho_v}{Y_v}\right) ln\left(\frac{1 - Y_{v,i}}{1 - Y_{v,b}}\right) \theta_{fog} \theta_{suc} \tag{6}$$

where $\dot{m}''_{v,i}$ is the interfacial condensation mass flux, x is the distance from the inlet, ρ_v is the vapor density, and Y_v is the mean vapor mass fraction. $Y_{v,i}$ and $Y_{v,b}$ are the mass fractions of vapor at the interface and in the bulk gas, respectively. θ_{fog} and θ_{suc} are the correction factors for fog formation and the suction effect, respectively.

2.2 Liquid film model

The liquid film model is a mechanistic model that calculates the liquid film thickness and velocity profile corresponding to the liquid film mass flow rate when the liquid condensate generated by condensation flows down the wall. The momentum equation within the liquid film is as follows [8]:

$$\frac{d}{dy}\left[(\nu_l + E)\frac{dU_l}{dy}\right] - \frac{1}{\rho_l}\frac{dP}{dz} + gsin\theta = 0 \tag{7}$$

where ν_l is the kinematic viscosity of the liquid, E is the eddy diffusivity of momentum for turbulent mixing, U_l is the liquid velocity, ρ_l is the liquid density, P is the pressure, z is the streamwise coordinate, g is the gravitational acceleration, and θ is the inclination angle of the wall.

The interfacial shear stress is defined by the difference between the gas bulk velocity and the interfacial velocity as follows:

$$\tau_i = \frac{1}{2} f_c \rho_b (u_b - u_i)^2 \tag{8}$$

where τ_i is the interfacial shear stress, f_c is the interfacial friction factor, ρ_b is the bulk gas density, u_b is the bulk gas velocity, and u_i is the interfacial velocity.

The film thickness δ_f is determined to satisfy the given film mass flow rate per unit width Γ_f. For this, the flow rate condition is defined in a dimensionless form as follows:

$$\frac{\Gamma_f}{\mu_l} = \int_0^{\delta_f^*} U_l^* \, dy^* \tag{9}$$

where μ_l is the dynamic viscosity of the liquid. U_l^*, δ_f^*, and y^* are the dimensionless liquid velocity, dimensionless film thickness, and dimensionless distance from the wall, respectively.

2.3 Model formulation for condensation of superheated steam

During the initial phase of an MSLB, the containment atmosphere can become superheated. According to the experimental study on superheated steam condensation by Murase et al. [9], the latent heat transfer during condensation of superheated steam was found to be nearly identical to that during condensation of saturated

steam. Based on this experimental evidence, the following relationship holds under superheated-steam conditions:

$$\dot{m}''_{v,sat} h_{fg} = \dot{m}''_{v,sh} h^*_{fg} \quad (10)$$

where $\dot{m}''_{v,sat}$ and $\dot{m}''_{v,sh}$ are the condensation mass fluxes under saturated and superheated conditions, respectively. h_{fg} and h^*_{fg} are the effective latent heats for saturated and superheated condition, respectively.

These effective latent heats are defined as:

$$h_{fg} = h_{g,sat} - h_{f,i} \quad (11)$$
$$h^*_{fg} = h_g(T_b) - h_{f,i} \quad (12)$$

where $h_{g,sat}$ is the specific enthalpy of saturated vapor, $h_{f,i}$ is the specific enthalpy of saturated liquid at the interface temperature, and $h_g(T_b)$ is the specific enthalpy of superheated vapor at the bulk temperature T_b.

Therefore, the condensation mass flux under superheated conditions is reduced as follows:

$$\dot{m}''_{v,sh} = \dot{m}''_{v,sat} \frac{h_{g,sat} - h_{f,i}}{h_g(T_b) - h_{f,i}} \quad (13)$$

2.3 Solution method

The overall solution consists of a coupled iterative procedure that converges the interface temperature in the condensation model and the film flow rate in the liquid-film model, as summarized in Fig. 2. First, an initial guess for the interface temperature T_i is specified. Using the current T_i, thermophysical properties in the diffusion layer and at the interface are updated.

The condensation mass flux is then evaluated by recalculating the boundary-layer thickness and turbulent diffusivity with the updated properties, followed by computing the vapor mass flux. The resulting condensation mass flux is passed to the liquid-film model as the liquid-film mass flow rate. In the liquid-film solver, the film thickness and interfacial shear condition are converted to a dimensionless form, the dimensionless velocity profile is computed, and the film thickness is iteratively updated until the flow rate is converged. After convergence, the film thickness, liquid-film velocity profile, and interfacial shear stress are obtained and used to account for the film thermal resistance in the heat-flux calculation.

Finally, the convergence of T_i is checked. If T_i is not converged, the procedure returns to the property-update step and repeats the coupled calculation. Once T_i converges, the total heat flux is obtained.

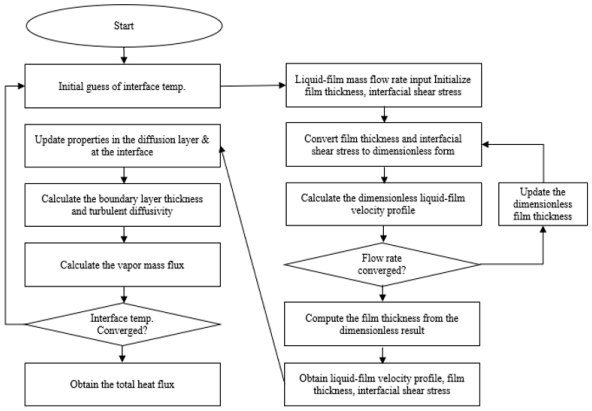

Fig. 2. Solution of the coupled condensation-liquid film model

3. Result

In this section, the developed model was validated using forced-convection flat plate condensation experiments, including COPAIN [10], CONAN [11], and SETCOM [12]. Table 1 shows the key specifications of the selected runs from each experiment.

Table I: The key specifications for condensation tests.

Test name	SETCOM	CONAN	COPAIN	
Test number	TEST 1	P10T30V25	P0242	P0441
Pressure (bar)	1.01	1.02	4.46	1.02
Bulk Temp (K)	353.15	348.75	422.5	353.2
Velocity (m/s)	4.68	2.57	2.0	3.0
Wall Temp (K)	283.15	303.55	304.3	307.4
AMF	0.65	0.716	0.99	0.767
Total Length (m)	6	2	2	

The Mean Percentage Error (MPE) was introduced to quantitatively evaluate the model error:

$$MPE(\%) = \frac{1}{N} \sum_{i=1}^{N} \frac{q''_{model}(x_i) - q''_{exp}(x_i)}{q''_{exp}(x_i)} \cdot 100 \quad (14)$$

where N is the total number of experimental data points, $q''_{model}(x_i)$ is the calculated local heat flux from the model at position x_i, and $q''_{exp}(x_i)$ is the measured local heat flux from the experiment at position x_i.

3.1 Saturated steam

Figs. 3 and 4 show the comparison of the heat flux between the new coupled model and the experimental data for SETCOM TEST 1 and CONAN P10T30V25, respectively. The new coupled model showed overall good agreement with the experimental data under both saturated-steam conditions, and the average MPE values were calculated to be 5.84% for SETCOM TEST 1 and -18.21% for CONAN P10T30V25. These results indicate that the experimental heat flux was predicted reasonably well under saturated-steam conditions. In addition, under these conditions, gas-side mass transfer resistance is dominant due to the presence of noncondensable gas, and thus the introduction of the liquid-film model does not significantly affect the overall heat-flux prediction.

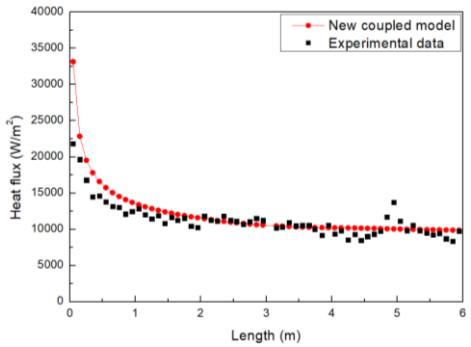

Fig. 3. Local heat flux comparison for SETCOM TEST 1

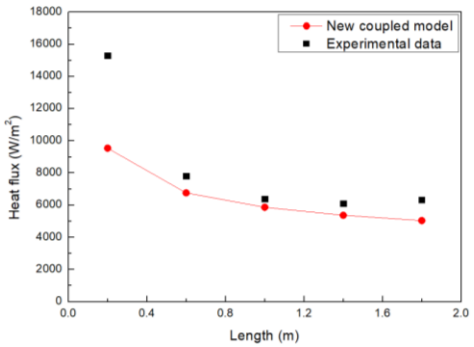

Fig. 4. Local heat flux comparison for CONAN P10T30V25

3.2 Superheated steam

Figs. 5 and 6 show the comparison results of the heat flux for COPAIN P0242 and COPAIN P0441, respectively. The average MPE values of the new coupled model were calculated to be -4.25% for COPAIN P0242 and 0.47% for COPAIN P0441, which correspond to similar or improved predictions relative to the experimental data compared with those of the condensation model [4], which showed -4.86% and 4.98%, respectively. In particular, the improvement achieved by the new coupled model was more pronounced for COPAIN P0441. In contrast, COPAIN P0242 had a very high air mass fraction of 0.99, so that sensible heat transfer was dominant over condensation latent heat transfer. Therefore, the introduction of the liquid-film model had only a limited effect on the overall heat-flux prediction, and no significant difference was observed between the two models.

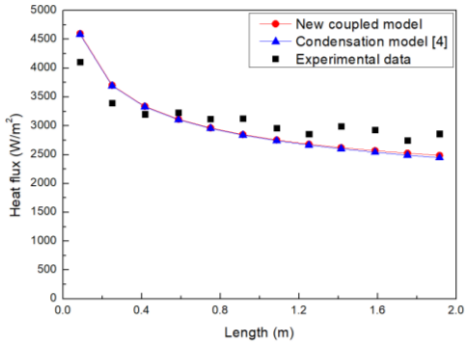

Fig. 5. Local heat flux comparison for COPAIN P0242

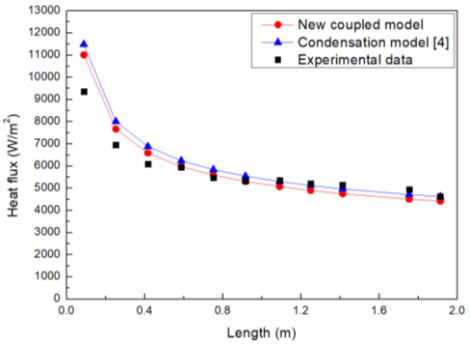

Fig. 6. Local heat flux comparison for COPAIN P0441

4. Conclusions

In this study, a new coupled model was developed by coupling a mechanistic condensation model with a liquid-film model for forced-convection condensation on a vertical flat plate, and the model was further extended to superheated-steam conditions. The proposed model was constructed so that the condensation mass flux calculated at the interface is consistently linked with the streamwise liquid-film flow, allowing the film thickness and thermal resistance to be reflected in the heat-flux calculation. In addition, under superheated-steam conditions, an effective latent heat concept was introduced to represent the heat-transfer characteristics in which sensible cooling and condensation latent heat transfer act simultaneously.

Comparison with experimental data showed that the proposed model provided overall good predictive performance under both saturated- and superheated-steam conditions, and that the interaction between condensate-film development and heat transfer was more directly reflected, particularly under superheated-steam conditions. These results indicate that the present model goes beyond a simple extension of the existing condensation analysis and provides a more physically consistent framework for representing the coupled effects of condensation mass transfer, liquid-film development, and wall heat transfer. Therefore, the proposed model can contribute to extending the

applicability of mechanistic condensation analysis to saturated- and superheated-steam mixture conditions relevant to containment thermal-hydraulic analysis.

Acknowledgements

This research was supported by the National Research Foundation of Korea grant funded by the Korean Government (MSIT) (No. RS-2022-00144494), and by the Nuclear Safety Research Program through the Regulatory Research Management Agency for SMRs (RMAS) and the Nuclear Safety and Security Commission (NSSC) of the Republic of Korea (No. RS-2024-00509653).

REFERENCES

[1] F. P. Incropera et al, D. P. DeWitt, T. L. Bergman, and A. S. Lavine, "Principles of Heat and Mass Transfer", 8th ed., Wiley, NJ, 2017.
[2] J. Tills, A. Notafrancesco, and J. Phillips, “Application of the MELCOR Code to Design Basis PWR Large Dry Containment Analysis”, SAND2009-2858, Sandia National Laboratories, Albuquerque, NM, 2009.
[3] A. J. Szukiewicz, “Interim staff position on environmental qualification of safety-related electrical equipment”, U.S. Nuclear Regulatory Commission, NUREG-0588 Rev. 1, 1981.
[4] J. Yu, Development of a Mechanistic Model for Analyzing Condensation Heat Transfer on Passive Heat Sinks within the Containment, M.S. thesis, Graduate School, Sejong University, Seoul, Korea, Feb. 2025.
[5] A. M. O. Smith, T. Cebeci, Numerical Solution of the Turbulent Boundary-Layer Equations, Douglas Aircraft Company, Douglas Aircraft Division, 1967
[6] T. Cebeci, Behavior of Turbulent Flow near a porous wall with pressure gradient, American Institute of Aeronautics and Astronautics Journal, Vol.8(12), p. 2152-2156, 1970
[7] J. Yu, J. H. Kang, H. J. Kim, and Y.-G. Lee, “A mechanistic model for forced convective condensation of steam with noncondensable gas on a vertical flat surface”, International Communications in Heat and Mass Transfer, Vol.175, 111124, 2026.
[8] S.M. Ghiaasiaan, Two-phase Flow, Boiling and Condensation, Cambridge University Press, New York, 2008.
[9] M. Murase et al., “Condensation heat transfer for downward flows of superheated steam-air mixture in a circular pipe”, Nuclear Engineering and Design 371, 110948, 2021.
[10] X. Cheng et al., Experimental Data Base for Containment Thermal hydraulic Analysis, Nuclear Engineering and Design, Vol.204, p. 267-284, 2001
[11] L. Vyskocil, J. Schmid, J. Macek, CFD Simulation of Air steam Flow with Condensation, Nuclear Engineering and Design. Vol.279, p. 147–157, 2014
[12] S. Kelm et al., Development of a Multi-dimensional Wall function Approach for Wall condensation, Nuclear